# Effect of Humpback Whale-like Leading-Edge Protuberances on the Low Reynolds Number Airfoil Aerodynamics

**M. M. Zhang, G. F. Wang and J. Z. Xu**

**Abstract** An experimental investigation of airfoil aerodynamics control at a low Reynolds number of $5 \times 10^4$ was conducted within the attack angle $\alpha$ of 0–90° using a leading-edge protuberance technique. The essence of the technique is to manipulate flow around the airfoil through the effect of a humpback whale-like leading edge. Whereas the mean lift force, drag force, and lift-to-drag ratio were measured using a 3-component force balance, the flow was mainly documented using a particle image velocimetry (PIV). The sinusoidal protuberances effectively suppressed the airfoil stall, although the corresponding aerodynamic performances were impaired to some extent. Meanwhile, the control significantly improved the airfoil aerodynamics in the post-stall $\alpha$ region, i.e., $16^\circ < \alpha < 70^\circ$, leading to a maximum 25.0 and 39.2 % increase in lift coefficient and lift-to-drag ratio, respectively, and maximum 20.0 % decrease in drag coefficient. The flow physics behind the observations were discussed.

**Keywords** Airfoil aerodynamics · Leading-edge protuberance · Stall

## 1 Introduction

Aerodynamic of airfoils operated at a low chord Reynolds number, i.e., $10^4 < \mathrm{Re}_c < 10^5$, has recently gained an increasing importance within the application fields of microair vehicles, small unmanned air vehicles, and small wind

The project was funded by NNSFC and MOST with Grant Nos. 51222606, 2010DFA62830, and CAS Hundred Talent Program.

M. M. Zhang (✉) · G. F. Wang · J. Z. Xu
Institute of Engineering Thermophysics, Chinese Academy of Sciences, No. 11 Beisihuan Road, Beijing 100190, People's Republic of China
e-mail: mmzhang@mail.etp.ac.cn

Y. Zhou et al. (eds.), *Fluid-Structure-Sound Interactions and Control*,
Lecture Notes in Mechanical Engineering, DOI: 10.1007/978-3-642-40371-2_15,

turbines. Nevertheless, the airfoils in this low $Re_c$ range are often subject to flow separation and even stall, resulting in poor aerodynamic performances and shortened fatigue lives. Therefore, effective control methods must be took to address this. Recently, a so-called leading-edge protuberance technique, inspired by the humpback whale flipper with rounded tubercles interspersed along its leading edge, has been given more and more attention. Within the last decade, many research works have been performed to investigate the effects of tubercles on the airfoil aerodynamic and hydrodynamic and good performances have been reported (Fish and Lauder 2006; Miklosovic et al. 2007; Johari et al. 2007; Goruney and Rockwell 2009; van Nierop et al. 2008). Even so, the detailed understanding of flow physics behind it is still very lacking, which may hinder the technique to be applied in the future. To this end, this paper presents an experimental study to investigate the nature of the modified airfoil aerodynamics by the presence of protuberances at low $Re_c$.

## 2 Experimental Details

Experiments were conducted in an open-loop wind tunnel with a test section of 0.5 × 0.5 × 2 m at Tsinghua University. The detailed setup was shown in Fig. 1. Two rectangular aluminum full-span $NACA63_4$-021 airfoils, i.e., a wavy airfoil with a sinusoidal leading edge (mimicking the cross-section to the flipper of a humpback whale) and a baseline airfoil with smooth leading edge, were chosen to be the test models. The mean $C_L$, $C_D$, and $L/D$ were measured using a 3-component force balance as $\alpha$ varied from $0^\circ$ to $90^\circ$, and the detailed flow structure is documented using particle image velocimetry (PIV). Measurements were carried out at a typical freestream velocity $U_\infty = 7.5$ m/s, corresponding to $Re_c$ of $5.0 \times 10^4$.

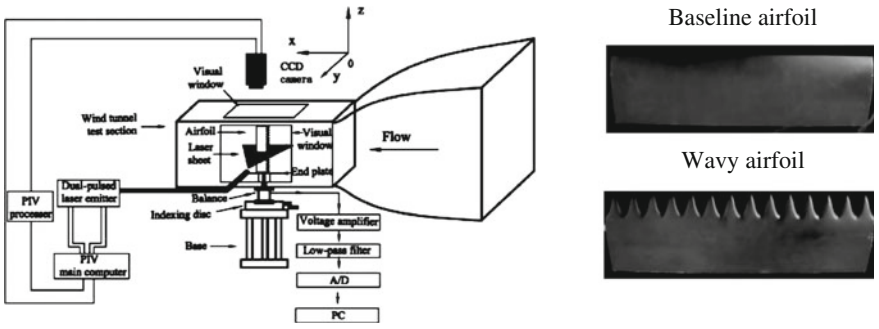


**Fig. 1** Experimental setup

## 3 Results and Discussion

### 3.1 Effect on Airfoil Aerodynamics

Figure 2 presents the dependences of the blockage-corrected mean $C_L$, $C_D$, and lift-to-drag ratio ($L/D$) on $\alpha$. Stall occurred at $\alpha = 13^{\circ}$, and then, $C_L$ displays another maximum at $\alpha = 45^{\circ}$. Compared with the baseline airfoil, all aerodynamic coefficients tend to be stable up to $\alpha = 3^{\circ}$. After that, as $3^{\circ} < \alpha \leq 16^{\circ}$, $C_L$ and $L/D$ evidently decrease (Fig. 2a, c) while $C_D$ mildly increases (Fig. 2b); the flow for the wavy airfoil case seems to not stall in the traditional sense of a rapid increase and thereafter a significant decrease in $C_L$, but $C_L$ gradually rises with $\alpha$, indicating the effectiveness of the passive control on inhibiting stall. The analogical phenomena on impairing the stall as well as detrimental to airfoil aerodynamics at the same time by leading-edge protuberances were also previously observed at the order of $Re_c$ magnitude of $10^5$ (Miklosovic et al. 2007; Johari et al. 2007). Moreover, the wavy airfoil exhibits rather good aerodynamic characteristics even when $\alpha$ varies from $16^{\circ}$ to $70^{\circ}$, resulting in the maximum 25.0 and 39.2 % increase in $C_L$ and $L/D$, respectively, and the maximum 20.0 % decrease in $C_D$, indicated in Fig. 2a–c.

### 3.2 Modified Stall Flow

To uncover the flow physics behind, two typical attack angle cases within stall and post-stall regions, i.e., $\alpha = 13^{\circ}$ and $40^{\circ}$, were selected for the following analysis. Figure 3a shows the contours of time-mean vorticity in $x$–$y$ plane out of 500 PIV images at $\alpha = 13^{\circ}$. The images for wavy airfoil cases were individually captured through the neighboring trough and peak location, which are near the airfoil mid-span. Clearly, flow separates at about $1/3c$ from the leading edge of the baseline airfoil. Once the wavy airfoil is introduced, flow in the trough-plane separates a little earlier while flow in the peak-plane adheres to the suction surface longer; the separated flow in the trough-plane reattaches to the suction surface and then moves toward the trailing edge for a while before leaving the surface again, resulting in

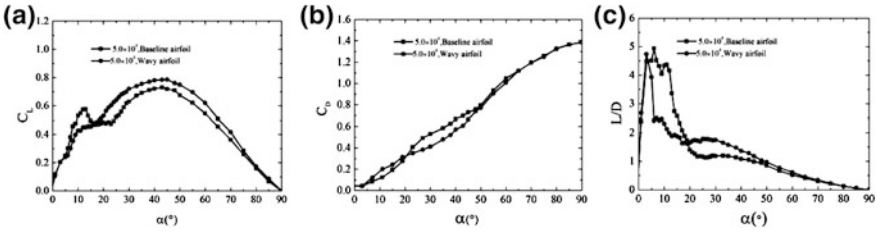


**Fig. 2** Airfoil aerodynamics with and without control

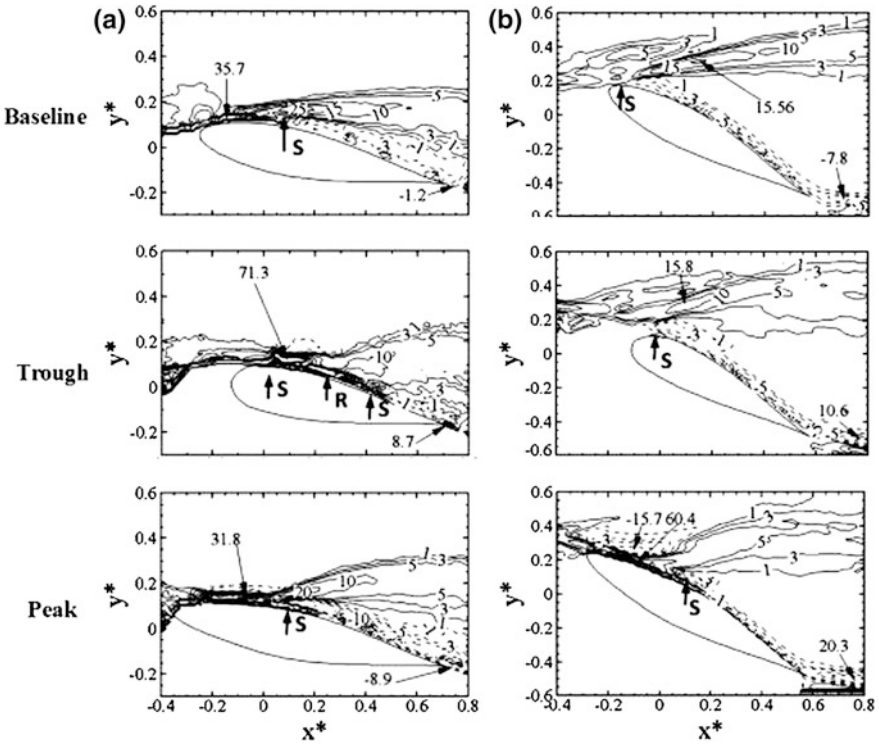


**Fig. 3** Contours of mean streamwise vorticity: **a** $\alpha = 13^{\circ}$; **b** $\alpha = 40^{\circ}$

much stronger separation than the baseline airfoil. Moreover, the typical averaged vorticity contours in $y$–$z$ plane at $x/c = 0.35$ (Fig. 4a) indicate that a pair of counter-rotating vortices are generated near each protuberance configuration, whose generation and subsequent mixing within neighboring valley region (Fish and Lauder 2006; Miklosovic et al. 2007; Johari et al. 2007; Goruney and Rockwell 2009; van Nierop et al. 2008) may partially account for more attached flow in the peak-plane as well as early separated and thereafter reattached flow in the trough-plane.

From another point of view, the typical profiles of mean streamwise velocity $\overline{U}^*$ above suction side at $\alpha = 13^{\circ}$ (Fig. 5a) show that the laminar flow separation occurs near $x/c = 0.1$ for the baseline case. In contrast, the separation takes place earlier for the trough case, and the reversed flow due to laminar separation successively weakens from $x/c = 0.1$ to 0.2 and quickly disappears between $x/c = 0.2$ and 0.3, suggesting that the flow transits and then reattaches to the airfoil surface again within the two $x/c$ ranges, respectively. The reversed flow appears again near $x/c = 0.4$, implying that the reattached turbulent boundary layer separates as $x > 0.4c$. The boundary thickness is about $0.12c$ at $x/c = 0.3$ and suddenly jumps to more than two times in magnitude ($0.25c$) at $x/c = 0.4$, which seemingly states

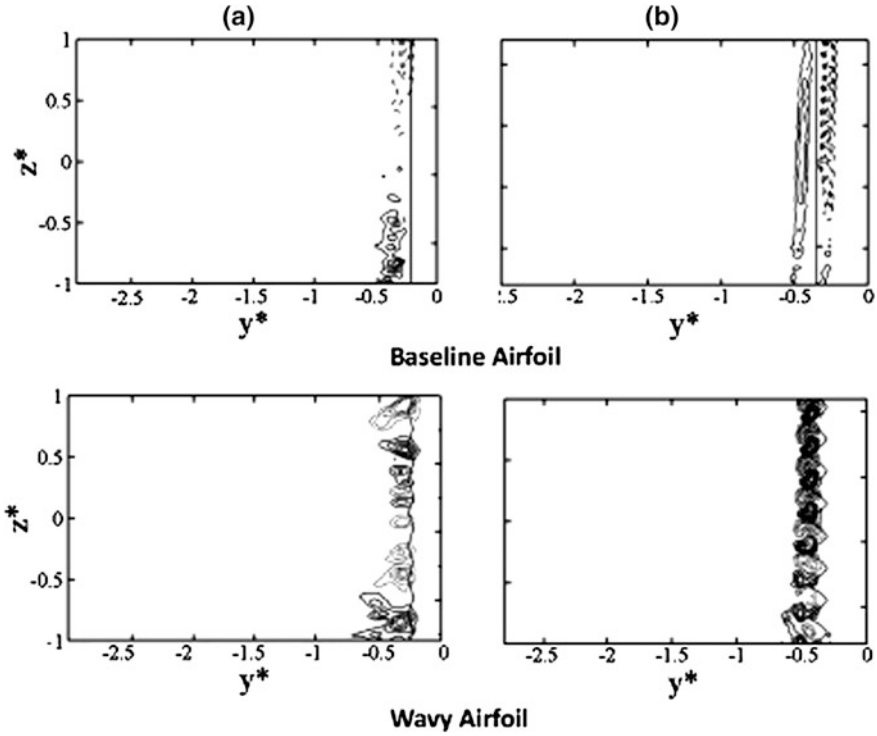


**Fig. 4** Contours of mean lateral vorticity: **a** $\alpha = 13^{\circ}$; **b** $\alpha = 40^{\circ}$

the thickened turbulent boundary layer due to the generation of streamwise vortices may be responsible for the detachment of turbulent flow in the trough-plane, consistent with the statements of Lissaman (1983). For the peak case, the occurrence of reversed flow moves backward to a location between $x/c = 0.1$ and $x/c = 0.2$, corresponding to a postponed laminar separation. Interestingly, such laminar separation in the peak-plane seems to be a little stronger than the baseline case near trailing edge, and the spanwise mixing of streamwise vortices at some distance behind airfoil leading edge may account for the extension of flow separation area.

Recalling that the aerodynamics of the wavy airfoil becomes worse in contrast to the baseline airfoil in the stall region (Fig. 2a–c, $3^{\circ} < \alpha \leq 16^{\circ}$), it implies that the enhanced separation originated from the complicated flow modification in the trough-plane might be responsible for the worse airfoil performance. This may further change the variation of $C_L$ with $\alpha$, leading to the impairment of airfoil stall.

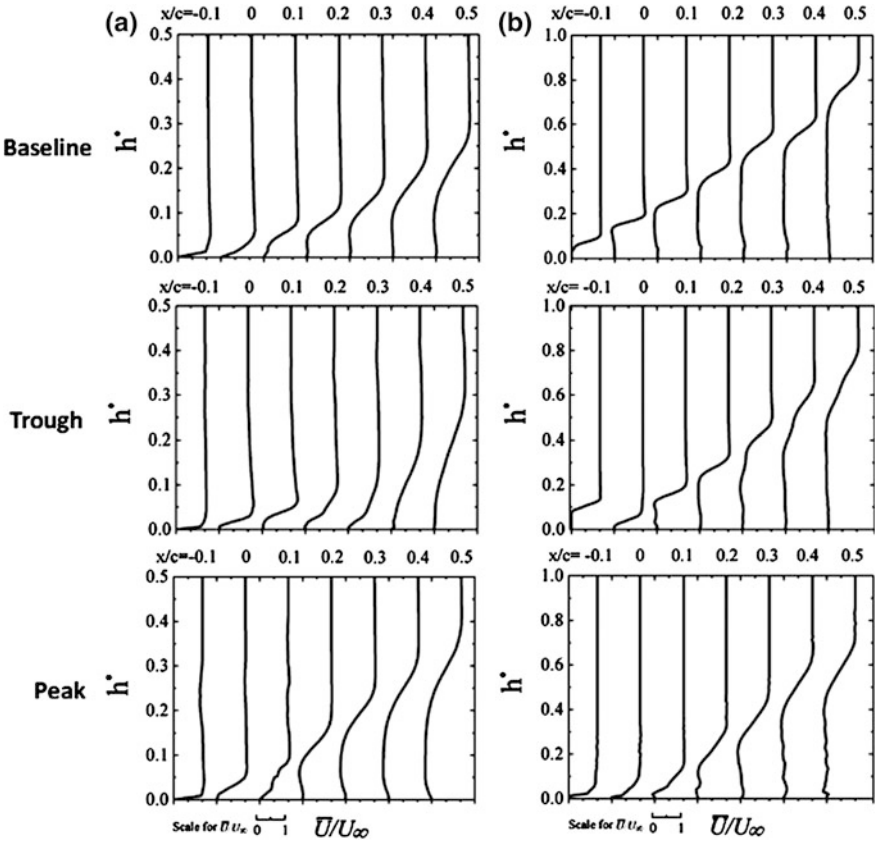


**Fig. 5** Mean streamwise velocity profiles of boundary layer: **a** $\alpha = 13^{\circ}$; **b** $\alpha = 40^{\circ}$

## *3.3 Modified Post-stall Flow*

For the typical post-stall case at $\alpha = 40^{\circ}$, the flow in the trough-plane tends to separate from the leading edge a little more seriously than the baseline case. Oppositely, the flow in the peak-plane still attaches to the suction side for a rather long distance (Fig. 3b), originated from the more generated vortex strengths in the peak-plane (Fig. 4b) to resist the negative pressure gradient and thus more attached flow than the baseline case, which may play a critical role in the improvements for the post-stall airfoil aerodynamics. Correspondingly, compared with the baseline airfoil case, the typical $\overline{U}^*$-profile (Fig. 5b) displays that the reversed flow pattern in the trough-plane does not change very much, while it is evidently impaired for the peak case. These results quantitatively point out that the impairment of flow separation and thus improvement of airfoil aerodynamics in post-stall originate from the effect of streamwise vortices induced by leading-edge protuberances.

## 4 Conclusions

The effects of sinusoidal leading-edge protuberances on two-dimensional full-span airfoil aerodynamics were experimentally investigated at low $Re_c$ of $5.0 \times 10^4$: (1) the airfoil stall was effectively inhibited while the post-stall airfoil aerodynamics was significantly improved in terms of $C_L$, $C_D$, and $L/D$. (2) In contrast with the baseline airfoil, the original stalled flow over trough section is subject to a series of complicated processes due to the protuberances-induced streamwise vortices, including laminar separation, laminar/turbulence transition, turbulent reattachment, and turbulent boundary layer detachment, leading to lessened lift as well as airfoil aerodynamics and an effective impairment in stall. (3) The post-stall airfoil performances were mainly manipulated by the flow over peak sections of protuberances, which remained attached well within a wide post-stall $\alpha$ range due to much stronger streamwise vortices, attributing to greatly enhanced momentum transfer and the corresponding significantly improved airfoil aerodynamics.

## References

Fish FE, Lauder GV (2006) Passive and active flow control by swimming fishes and mammals. Annu Rev Fluid Mech 38:193–224

Goruney T, Rockwell D (2009) Flow past a delta wing with a sinusoidal leading edge: near-surface topology and flow structure. Exp Fluids 47:321–331

Johari H, Henoch C, Custodio D, Levshin A (2007) Effects of leading-edge protuberances on airfoil performance. AIAA J 45(11):2634–2642

Lissaman PBS (1983) Low-reynolds-number airfoils. Annu Rev Fluid Mech 15:223–239

Miklosovic DS, Murray MM, Howle LE (2007) Experimental evaluation of sinusoidal leading edges. J Aircraft 44(4):1404–1407

Van Nierop EA, Alben S, Brenner MP (2008) How bumps on whale flippers delay stall: an aerodynamic model. Phy Rev Lett 100:054502